IAI
Journals.ASM.org

Limited Model Antigen Expression by Transgenic Fungi Induces Disparate Fates during Differentiation of Adoptively Transferred T Cell Receptor Transgenic CD4$^+$ T Cells: Robust Activation and Proliferation with Weak Effector Function during Recall

Marcel Wüthrich,[a] Karen Ersland,[a] John C. Pick-Jacobs,[a] Benjamin H. Gern,[a] Christopher A. Frye,[a] Thomas D. Sullivan,[a] Meghan B. Brennan,[a] Hanna I. Filutowicz,[a] Kevin O'Brien,[c] Keegan D. Korthauer,[d] Stacey Schultz-Cherry,[c] and Bruce S. Klein[a,b,c]

Departments of Pediatrics,[a] Internal Medicine,[b] Medical Microbiology and Immunology,[c] and Biostatistics and Medical Informatics,[d] University of Wisconsin Medical School, University of Wisconsin Hospital and Clinics, Madison, Wisconsin, USA

CD4$^+$ T cells are the key players of vaccine resistance to fungi. The generation of effective T cell-based vaccines requires an understanding of how to induce and maintain CD4$^+$ T cells and memory. The kinetics of fungal antigen (Ag)-specific CD4$^+$ T cell memory development has not been studied due to the lack of any known protective epitopes and clonally restricted T cell subsets with complementary T cell receptors (TCRs). Here, we investigated the expansion and function of CD4$^+$ T cell memory after vaccination with transgenic (Tg) *Blastomyces dermatitidis* yeasts that display a model Ag, Eα-mCherry (Eα-mCh). We report that Tg yeast led to Eα display on Ag-presenting cells and induced robust activation, proliferation, and expansion of adoptively transferred TEa cells in an Ag-specific manner. Despite robust priming by Eα-mCh yeast, antifungal TEa cells recruited and produced cytokines weakly during a recall response to the lung. The addition of exogenous Eα-red fluorescent protein (RFP) to the Eα-mCh yeast boosted the number of cytokine-producing TEa cells that migrated to the lung. Thus, model epitope expression on yeast enables the interrogation of Ag presentation to CD4$^+$ T cells and primes Ag-specific T cell activation, proliferation, and expansion. However, the limited availability of model Ag expressed by Tg fungi during T cell priming blunts the downstream generation of effector and memory T cells.

Diseases due to fungi represent a growing public health problem that demand new treatments and methods of vaccine prevention (8). The rational design of vaccines against fungi requires an understanding of the elements of antifungal immunity. Cellular immunity is pivotal in acquired resistance to fungal infections and is organized into clonal populations of antigen (Ag)-specific CD4$^+$ T cells (8, 30, 40). The ability to track, enumerate, and characterize Ag-specific T cells precisely requires knowledge of the Ag peptide. With such information, peptide-major histocompatibility complex (MHC) tetramers and T cell receptor (TCR) transgenic (Tg) mice have been used to track and enumerate Ag-specific T cells *ex vivo* to circumvent *in vitro* expansion or distortion of immune responses.

Reagents are available to precisely study T cell immunity with model agents such as lymphocytic choriomeningitis virus and *Listeria* (9, 22), but the study of most other pathogens is not readily approachable with these high-resolution methods. For the systemic dimorphic fungi, no T cell Ag epitopes have been elucidated to provide the tools to address this gap in knowledge. To bridge this gap, we engineered heterologous Ag and epitopes into a vaccine strain of a pathogenic fungus to let us induce, track, quantify, characterize, and functionally analyze adoptively transferred TCR Tg T cells specific for the foreign Ag in vaccinated animals.

Blastomycosis is a systemic infection due to the dimorphic fungus *Blastomyces dermatitidis*. We have created a live attenuated vaccine against lethal experimental infection (38). The vaccine induces sterilizing immunity that is mediated by CD4$^+$ T cells, although the protective antigen remains unknown. Still, this model and the potent activity of these CD4$^+$ T cells offer the chance to elucidate the requirements for inducing and maintaining antifungal CD4$^+$ T cells by vaccination. As a surrogate means to study the *in vivo* activation, proliferation, and maintenance of *Blastomyces*-specific CD4$^+$ T cells, we expressed model epitopes on the vaccine *B. dermatitidis* yeast using BAD1, an abundant surface protein, as a carrier. Yeast surface Ag display is thought to be one feature that promotes the generation of antifungal immune responses.

In other nonfungal models, the availability of Ag and the number of naïve T cell precursors in a host can affect the priming and development of CD4$^+$ effector and memory T cells (1, 27). However, little is known about the identity, cellular distribution, and expression levels of fungal T cell epitopes and how these factors influence the development of antifungal immunity. We report that expressing a model epitope such as Eα peptide on vaccine yeast induced the activation and proliferation of corresponding naïve, adoptively transferred TCR Tg TEa cells. We describe the experimental system and our results enabling the tracking of fungal Ag presentation to CD4$^+$ T cells and the corresponding Ag-specific T cell response during their earliest stages of activation, proliferation, and expansion. Interestingly, these antifungal T

Received 2 May 2011 **Returned for modification** 22 May 2011
Accepted 15 November 2011
Published ahead of print 28 November 2011
Editor: G. S. Deepe, Jr.
Address correspondence to Marcel Wüthrich, mwuethri@wisc.edu.

doi:10.1128/IAI.05326-11

cells ultimately failed to differentiate into potent effector cells and migrate to lung upon rechallenge. We propose that this functional deficit of antifungal TEa cells is likely due to an insufficient Ag threshold reached by the vaccine since addition of exogenous Eα peptide corrected the deficit.

MATERIALS AND METHODS

Mouse strains. Inbred strains of C57BL/6 mice (males 7 to 8 weeks old at the time of these experiments) and the T lymphocyte-specific Thy1.1 allele-carrying congenic C57BL/B6 strain B6.PL-Thy1^a/Cy (stock no. 000406) (12) were obtained from Jackson laboratories, Bar Harbor, ME. Two male TEa Tg mice of the C57BL/6J (B6; I-A^b, I-E$^-$) background (13, 15) expressing the Thy1.2 allele were generously provided by A. Y. Rudensky at the Howard Hughes Medical Institute, University of Washington. The Tg TCR in TEa mouse lymphocytes recognizes a peptide representing residues 52 to 68 of the I-Eα chain (Eα peptide) bound to class II I-A^b molecules. TEa Tg mice expressing the Thy1.1 allele were produced at the University of Wisconsin by backcrossing the original TEa males two times to wild-type B6 females expressing the congenic Thy1.1 marker and screened for the Thy1 allele and transgene. To identify the transgene-positive progeny, lymphocytes from peripheral blood were stained with phycoerythrin (PE)-Cy7-labeled anti-CD4, fluorescein isothiocyanate (FITC)-labeled anti-Vα2, and PE-labeled anti-Vβ6 antibodies (BD Pharmingen) and analyzed by fluorescence-activated cell sorter (FACS) analysis as previously described (15). *Blastomyces*-specific TCR Tg strain 1807 mice were generated in the Klein lab and described elsewhere (37, 42, 43). Strain 1807 mice were backcrossed to congenic Thy1.1-positive (Thy1.1$^+$) mice as described above. Mice were housed and cared for according to guidelines of the University of Wisconsin Animal Care Committee, who approved all aspects of this work.

Fungi and growth conditions. Strains used were ATCC 26199 (American Type Culture Collection) (16), a wild-type virulent strain, and the isogenic, attenuated mutant lacking BAD1, designated strain 55 (6). Isolates of *B. dermatitidis* were maintained as yeast on Middlebrook 7H10 agar with oleic acid-albumin complex (Sigma Chemical Co., St. Louis, MO) at 39°C.

Engineering yeast expressing the model antigenic epitopes Eα and 2W1S. Yeast cells expressing either Eα or 2W1S Ag epitopes were generated by *Agrobacterium*-mediated transformation using a binary plasmid expressing a three-way fusion of the epitope, the red fluorescent protein (RFP) mCherrry (mCh) (32), and a truncated version of BAD1. To streamline the generation of chimeric genes expressing different epitopes, an *Agrobacterium* binary plasmid that contains unique cloning sites and the *ccdB* gene inserted into the NcoI site in the truncated BAD1 gene was constructed. The *ccdB* gene aids in the cloning of sequences of choice by preventing *Escherichia coli* clones harboring nonrecombinant, parental plasmids from growing (3). Primers were obtained from Integrated DNA Technologies (Coralville, IA). PCR for cloning was done using Elongase (Invitrogen, Carlsbad, CA). The starting plasmid was a derivative of pBAD1-6H, containing the truncated tandem repeat sequence (ΔTR20) of BAD1 (5), called pΔ5-6H. The *ccdB* gene was PCR amplified from an Invitrogen Gateway cassette-containing plasmid using primers that added NcoI and AscI sites at the 5′ end of the forward primer, tdsP182 (GCGCCC ATGGCGCGCCTGGCCGGCCTACTAAAAGCCAGATAACAGT), and NcoI and SwaI at the 5′ end of the reverse primer, tdsP181 (GCGCCCA TGGGATTTAAATCGGCCGGCCAGTCGTTCGGCTTCATCT). Following PCR, the 800-bp fragment was digested with NcoI and ligated with pΔ5-6H plasmid DNA that had also been digested with NcoI, and the ligated DNA was electroporated into an *E. coli* strain permissive for growth with the *ccdB* gene, DB3.1 (35). Transformants were screened for the presence of the insert and correct orientation. In addition, the cloned plasmids were tested for a functional *ccdB* gene by electroporating them into the nonpermissive strain DH10β and finding that transformants were severely restricted in growth. The ΔTR20-*ccdB* chimeric gene was excised with XbaI (filled in) and EcoRI and moved into the *Agrobacterium* binary vector pCTK4 (28) at the HindIII (filled in) and EcoRI sites, creating plasmid pCTS33. A fragment containing the Eα epitope region of pTrc-Eα-RFP (encoding amino acids 52 to 68 and 6 flanking amino acids of the Eα protein [19, 31] and the mCherry RFP gene [32]) was generated using splicing overlap (SOE) PCR (23) with Eα forward primer tdsP202 containing an incorporated AscI site at its 5′ end (CGCGGGCGCGCCGA AGAATTTGCAAAGTT), SOE fusion Eα-mCherry (Eα-mCh) reverse primer tdsP216 (AACCTGGATGTCATGGAGGTGAGCAAGGGCGAG GAG), SOE fusion Eα-mCherry forward primer tdsP217 (CTCCTCGCC CTTGCTCACCTCCATGACATCCAGGTT), and the mCherry reverse primer tdsP218 with a SmaI site at its 5′ end (CGCGCCCGGGCCTTGT ACAGCTCGTCCAT). The fused fragment was digested with AscI and SmaI and ligated with pCTS33, which had been digested with AscI and SwaI, and the DNA was electroporated into *E. coli* strain DH10β. To create a 2W1S epitope-mCherry fusion, a 93-nucleotide (nt) oligomeric primer that contains sequence encoding the 14-amino-acid 2W1S epitope (29) flanked by 2 amino acids that match those flanking the comparable sequence of the Eα epitope and two glycine residue spacers was generated (composite amino acid sequence, GGSFEAWGALANWAVDSANLGG). In addition, this primer includes a 5′ end AscI site and 3′ end sequence for priming at the start of the mCherry sequence (tdsP615, GCGCGGCGCG CCGGCGGTAGCTTTGAGGCTTGGGGTGCACTGGCTAATTGGGCT GTGGACAGCGCTAACCTGGGCGGTGTGAGCAAGGGCGAG). Primer tdsP615 was used with tdsP618 (GGGCCTTGTACAGCTCGTCCAT) to amplify a cloned mCherry sequence and, in so doing, add the 2W1S epitope sequence. The fragment was digested with AscI, which cuts at the 5′ end of the fragment (the 3′ end was left blunt), and ligated to AscI- and SwaI-digested pCTS33. For both Eα and 2W1S, transformants were screened for plasmids with the new insert and sequenced to find those without PCR-induced mutations and to confirm that the Eα-mCherry or 2W1S-mCherry fragment had been inserted to create a single translational fusion in the ΔTR20 protein backbone. The plasmids were electroporated into *Agrobacterium tumefaciens* strain LBA1100 harboring the Ti plasmid pAL1100 (2, 10). Confirmed *A. tumefaciens* strains were used to transform yeast-phase cells of *B. dermatitidis* strain ATCC 26199 and strain 55, the BAD1-knockout derivative of ATCC 26199 (5, 35).

Screening and characterization of Tg yeast. Transformants of strain 55 were initially screened for production of the fusion protein using an overlay assay to detect secreted BAD1 (6) and subsequently analyzed by Western blotting with anti-BAD1 antibodies on yeast cell extracts to confirm that the fusion protein is the predicted size (5) (data not shown). Positive yeast cell lines were also screened for red fluorescence microscopically on an Olympus BX60 fluorescence microscope (Center Valley, PA) and by FACS analysis using the dichroic mirror at 595LP and the PE-Texas Red band-pass filter (6). Finally, the strains showing high expression of the Tg protein were also noted to have visibly pink/red colonies when plated on 7H10 medium, and this characteristic was used to ensure that yeast cells used for *in vivo* and *in vitro* experiments were expressing the Eα- or 2W1S-mCherry-ΔTR20 (truncated BAD1) fusion protein at high levels. To identify transformants with the highest transgene expression, we stained them with 1 μg of anti-BAD1 monoclonal antibody (MAb) DD5-CB4 (44) and goat anti-mouse IgG FITC-conjugated secondary antibody (1:200 dilution; Sigma) for 30 min and analyzed the yeast for maximal fluorescence in the FITC (BAD1) and PE-Texas Red (mCh) channels by FACS analysis. Tg ATCC 26199 yeast cells were identified by using the red color as an indication for transgene expression as described above.

Preparation of Eα-RFP from *E. coli*. The generation of recombinant *E. coli* expressing the Eα-RFP fusion protein containing the Eα and DsRed sequences, kindly provided by Marc Jenkins (Minneapolis, MN), was described elsewhere (19). Protein production was induced with 1 mM isopropyl-β-D-thiogalactopyranoside overnight, and the Eα-RFP fusion protein was purified from the bacterial lysate using either a chitin-bead affinity column (New England BioLabs) or an Ni^{2+} resin His-Bind column (Novagen).

Generation and use of Y-Ae antibody. The Y-Ae hybridoma was generously provided by Marc Jenkins (University of Minnesota) (19). Monoclonal antibody from ascites was ammonium sulfate precipitated, purified on protein A/G agarose according to the manufacturer's specifications for the isolation and purification of IgG (product 21001; Pierce Chemical, Rockford, IL), and quantified by measuring the optical density at 280 nm. The MAb was biotinylated using an EZ-Link *N*-hydroysulfosuccinimide long chain (sulfo-NHS-LC) kit (Thermo Fisher Scientific) according to the manufacturer's protocol. To detect Eα peptide-MHC class II (MHC-II) displayed in bone marrow-derived dendritic cells (BM-DCs), Y-Ae antibody was used at 50 to 100 μg per sample. Y-Ae staining was performed with a staining buffer of phosphate-buffered saline (PBS) containing 1% bovine serum albumin plus 2 mM EDTA.

Recombinant VSV-SED- and 2W1S-expressing *Listeria monocytogenes*. The recombinant vesicular stomatitis virus (VSV) containing a gene cassette encoding the ovalbumin-derived peptide SIINFEKL, the Eα peptide (amino acid residues 52 to 68), and DsRed (VSV-SED) was kindly provided by Leo Lefrancois (Storrs, CT) (4). The recombinant *Listeria monocytogenes* strain expressing the 2W1S peptide was kindly provided by Marc Jenkins (11).

Vaccinations with soluble Eα-RFP, 2W1S peptide plus LPS, Eα-mCh- and 2W1S-mCh-expressing yeast, and VSV-SED- and 2W1S-expressing *L. monocytogenes*. Unless otherwise stated, C57BL/6 mice were vaccinated subcutaneously (s.c.) at two sites, dorsally and at the base of the tail, using one injection of the following formulations, doses, and routes of delivery: recombinant yeast expressing Eα-mCh, 2W1S-mCh, or BAD1-null attenuated yeast was injected either live s.c. or in a heat-killed form intravenously (i.v.) using a dose range of 10^5 to 10^7 yeast per mouse. Soluble Eα-RFP from 0.8 μg to 100 μg recombinant protein was injected s.c. alone or as an emulsion with incomplete Freund's adjuvant (IFA). The 2W1S peptide (EAWGALANWAVDSA) was purchased from Biosynthesis, Lewisville, TX, and injected i.v. as a mixture containing 50 μg 2W1S peptide and 5 μg lipopolysaccharide (LPS; Sigma). VSV-SED was injected either i.v. using a dose of 10^5 PFU (4) or s.c. at a range of 10^5 to 10^8 PFU recombinant *L. monocytogenes* expressing 2W1S peptide, which was injected i.v. using a range of 10×10^6 to 100×10^6 live bacteria.

Adoptive transfer of Tg CD4$^+$ T cells and surface staining. Single-cell suspensions of splenocytes from TEa or 1807 mice (Thy1.1$^+$ background) were labeled with 5- and 6-carboxyfluorescein diacetate succinimidyl ester (CFSE; Molecular Probes) as described previously (33), and various numbers of labeled cells were injected i.v. into wild-type congenic Thy1.2$^+$ C57BL/6 male recipients. At various times after Ag injection, single-cell suspensions from draining inguinal and brachial lymph nodes of recipient mice were stained with monoclonal antibodies directed against the following surface markers; CD4, CD8, Thy1.1, CD44, CD62L, and B220 (as a dump marker). MAbs were obtained from BD Pharmingen (San Diego, CA) and eBioscience (San Diego, CA), and cytometry data were gathered with an LSRII flow cytometer (BD Biosciences, San Jose). Data were analyzed by using FlowJo software (Tree Star, Ashland, OR). The number of TEa and 1807 CD4$^+$ T cells in a lymph node was calculated by multiplying the percentage of Thy1.1$^+$ CD4$^+$ cells by the number of viable cells determined by trypan blue dye exclusion.

BrdU incorporation. On the day of challenge and daily thereafter, mice were given 2 mg of 5′-bromo-2-deoxyuridine (BrdU) in PBS by intraperitoneal (i.p.) injection. Four days later, the mice were sacrificed and T cells from the lung and mediastinal lymph node (MLN) were stained for surface markers and stained for BrdU incorporation using an FITC BrdU flow kit from BD Pharmingen, San Diego, CA.

Intracellular cytokine staining. Lung and draining lymph node cells were obtained as described previously (39). An aliquot of isolated cells was stained for surface CD4 and Thy1.1 to determine the percentage of transferred TCR Tg cells. The numbers of Tg cells per lung or lymph nodes were derived by multiplying the percentage of cells by the total number of cells per organ isolated. The rest of the cells were stimulated with anti-CD3 and anti-CD28 MAbs. After the 4- to 6-h stimulation, cells were stained for surface markers, fixed, permeabilized with a Cytofix/Cytoperm kit (BD Pharmingen), and stained with anticytokine antibodies as previously described (41, 45).

Peptide–MHC-II tetramer-based enrichment to detect 2W1S-specific endogenous T cells. The spleen and inguinal and brachial lymph nodes were harvested for each mouse analyzed. A single-cell suspension was prepared and enriched with PE-conjugated 2W1S tetramer as described previously (26, 27). The resulting enriched fractions were resuspended in 0.1 ml of sorter buffer, and a small volume was removed for cell counting, while the rest of the sample was stained with a cocktail of the following fluorescently labeled antibodies: CD3-FITC, 2W1S tetramer-PE, CD4-peridinin chlorophyll protein, CD44 Alexa 700, CD8 V780, and biotinylated B220, CD11c, and CD11b-Strep V450 (as a dump channel). The entire sample was collected on an LSRII flow cytometer and analyzed with FlowJo software using the gating strategy described previously (26, 27). The percentage of tetramer-positive events was multiplied by the total number of cells in the enriched fraction to calculate the total number of tetramer-positive cells in the organs harvested.

Cytokine protein measurements. Cell culture supernatants were generated in 24-well plates in 1 ml containing 2×10^5 TEa, OT-II, or naïve CD4$^+$ T cells and BM-DCs (1:1 ratio), 10 μM Eα peptide, or 10^5 Eα-RFP or TR20 yeast (38). Supernatants were collected after 48 h of coculture. Granulocyte-macrophage colony-stimulating factor (GM-CSF) and interleukin-2 (IL-2) (R&D System, Minneapolis, MN) were measured by enzyme-linked immunosorbent assay (ELISA) according to manufacturer specifications (detection limits, 0.05 ng/ml and 0.02 ng/ml, respectively).

Experimental infection. At 4 to 5 weeks postvaccination, mice were infected intratracheally (i.t.) with 2×10^3 to 2×10^4 wild-type strain ATCC 26199 or Eα-mCh-expressing ATCC 26199 yeast cells as described previously (38). At day 4 postinfection, coinciding with the peak of T cell influx (39, 40), the mice were sacrificed and lung T cells were analyzed by FACS analysis.

Statistical analysis. The number and percentage of activated, proliferating, or cytokine-producing T cells and differences in numbers of CFU were analyzed using the Wilcoxon rank test for nonparametric data (14) or the *t* test when data were normally distributed. Contractions of T cells (number of T cells at the burst of expansion versus during the memory phase) were analyzed by the two-way analysis of variance test. A *P* value of <0.05 is considered statistically significant.

RESULTS

Generation and characterization of transgenic *B. dermatitidis* yeast. To enumerate, characterize, and track Ag-specific T cells, we expressed the model epitope Eα (for which TCR Tg TEa mice are available) fused to mCherry (Eα-mCh) in the vaccine strain of *B. dermatitidis*. Eα-mCh protein is a recombinant 32-kDa chimeric fusion protein consisting of amino acids 46 to 74 of the I-E$^d\alpha$ MHC-II subunit at the N terminus and the red fluorescent protein mCherry at the C terminus (32). We hypothesized that chimeric Eα-mCh protein expressed on a backbone of the signal sequence and 10 copies of the BAD1 tandem repeat (Fig. 1A) would be delivered to the cell surface and stain the yeast red. We assessed Tg yeast by microscopy and FACS analysis. Eα-mCh yeast stained red (Fig. 1B and C) and expressed BAD1 at levels comparable to TR20 control yeast, whereas BAD1-null yeast failed to stain red or express BAD1 (Fig. 1C). Thus, our Tg yeast displayed chimeric Eα-mCh-BAD1 in and on the yeast cell.

We tested whether chimeric Eα-mCh-BAD1 on yeast is processed and presented by antigen-presenting cells (APCs). When the Tg yeast was added to bone marrow-derived DCs *in vitro*, the fungi were processed and the pEα–I-A^b complexes were displayed on the DC surface and detected by FACS analysis with Y-Ae MAb (Fig. 2A). The findings with Eα-mCh yeast were comparable to

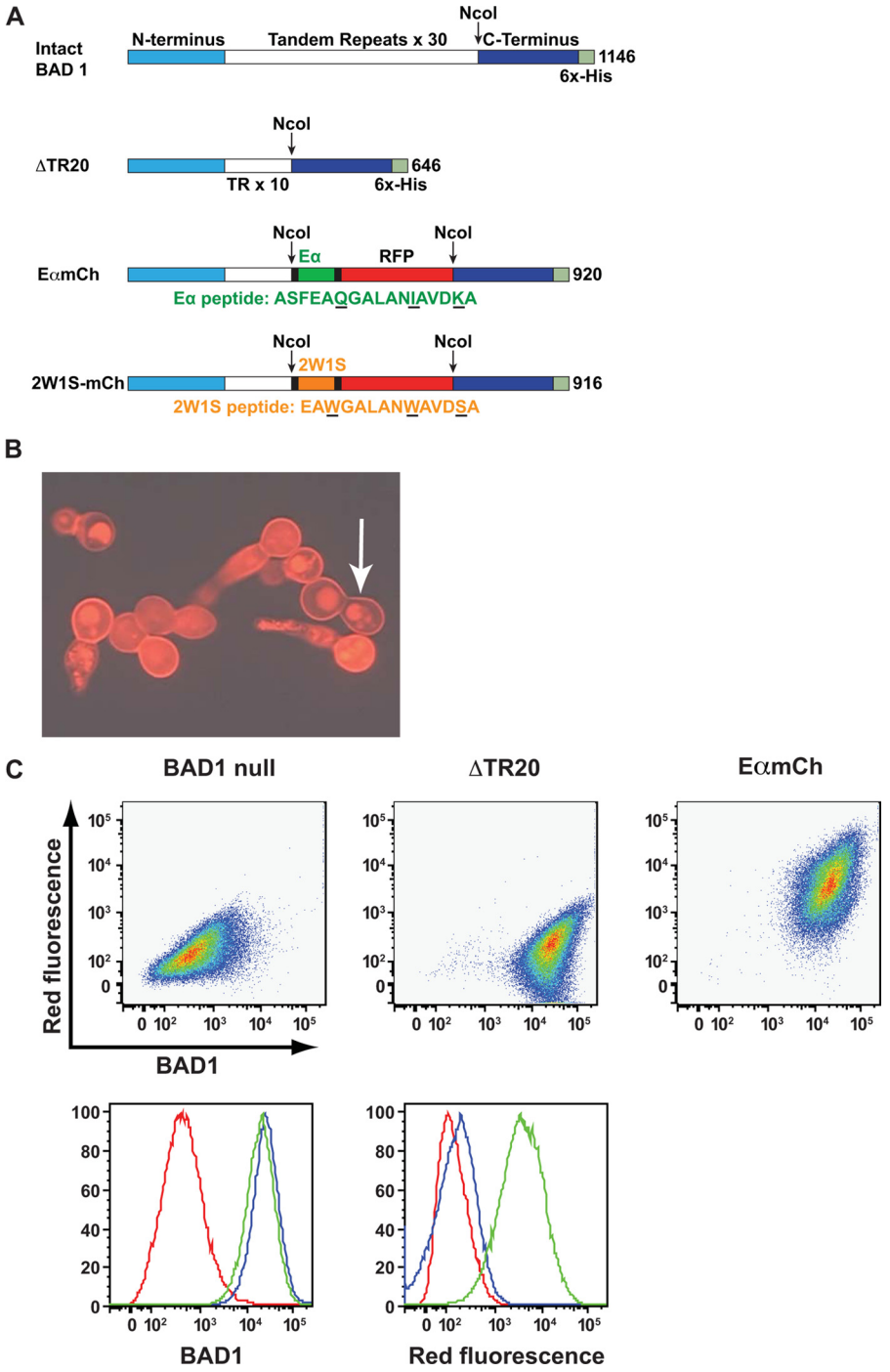

FIG 1 Tg yeast of *B. dermatitidis*. (A) Intact BAD1 (top) with 30 copies of the tandem repeat (white box) and ΔTR20 (2nd row), a derivative with 20 repeats deleted (5). We used BAD1 in ΔTR20, driven by its own promoter, as a fusion partner to make chimeric proteins with either the Eα or the 2W1S epitope fused to the RFP mCherry (25) and inserted in frame at the start of the C terminus (dark blue box; see Materials and Methods). The N-terminal BAD1 sequence (light blue) encodes a signal sequence for export, and the C terminus is needed for binding to the yeast cell wall. The antigenic peptides (green or orange box) with their flanking sequences (black) are shown. The construct name is on the left, the total amino acid length is given on the right, and the amino acid sequence of the epitope is given below in green or orange. The underlined amino acids are those that differ in the comparable sequence of Eα and 2W1S. Map domain lengths are not to scale. (B) Eα-mCh yeasts fluoresce red inside and on the cell wall (arrow). (C) BAD1-null (strain 55 [6]), ΔTR20, and Eα-mCh-expressing yeasts were stained and analyzed for BAD1 expression and red fluorescence by FACS analysis. The mean fluorescent intensity (MFI) for BAD1 expression on Eα-mCh yeast and TR20 yeast was 58 and 33 times higher, respectively, than that on BAD1-null yeast. The red fluorescence of Eα-mCh yeast was 25 times higher than that of TR20 and BAD1-null yeast, as measured by determination of the mean fluorescent intensity. The histogram depicts BAD1 expression (FITC) and red fluorescence (PE-Texas Red) for BAD1-null (red), ΔTR20 (blue), and Eα-mCh (green) yeasts.

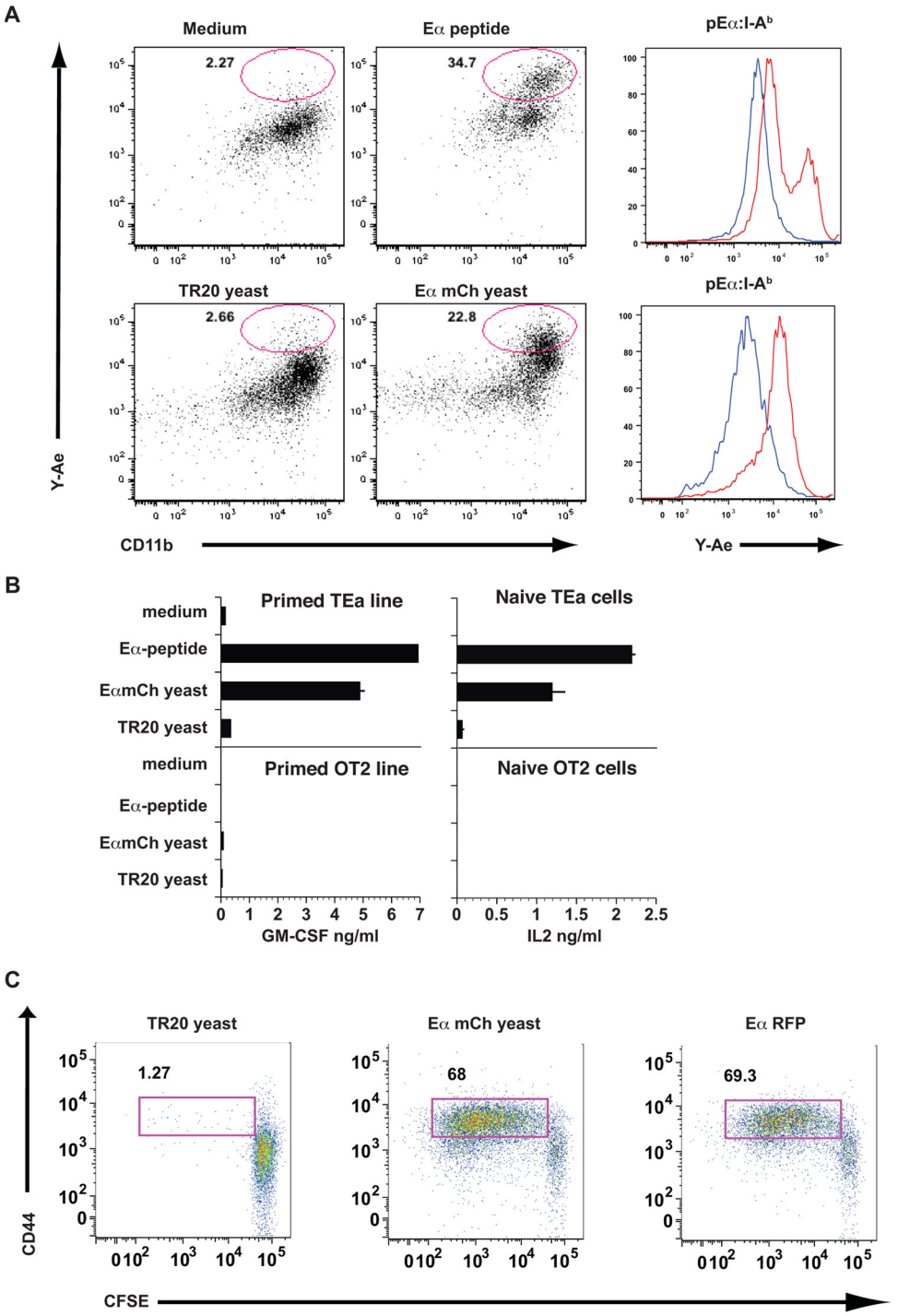

FIG 2 Yeast Eα peptide is processed and presented by DCs and stimulates TEa T cells *in vitro* and *in vivo*. (A) Bone marrow-derived DCs were cultured in medium alone, 30 μM Eα peptide, or 2×10^5 yeast cells (1:1 ratio). After 24 h, DCs were stained with anti-CD11b and Y-Ae MAbs and analyzed. Blue denotes Y-Ae display by DCs cultured with medium alone or ΔTR20 yeast. Red denotes Y-Ae staining by DCs cultured with Eα peptide or Eα-mCh yeast. (B) A TEa T cell line (2×10^5 cells/well) or naïve TEa T cells (10^6 cells/well) were cultured with DCs (1:1 ratio) and the stimuli shown for 48 h. Supernatants were tested for cytokine by ELISA for IL-2 and GM-CSF as standard measures of T cell activation. OT-II cells were from a T cell line (2×10^5 cells/well). (C) Thy1.2$^+$ wild-type mice got 5×10^6 Thy1.1$^+$ TEa cells i.v. and were vaccinated with Eα-RFP yeast or 50 μg Eα-RFP s.c. Four days later, nodes were taken and Thy1.1$^+$ T cells were assayed for proliferation (CFSE) and activation (CD44) by FACS analysis. The gates and percentages indicate the percentage of CFSE^{low} TEa cells that express high levels of CD44. The data are representative of 4 mice/group, and the experiment was repeated three times.

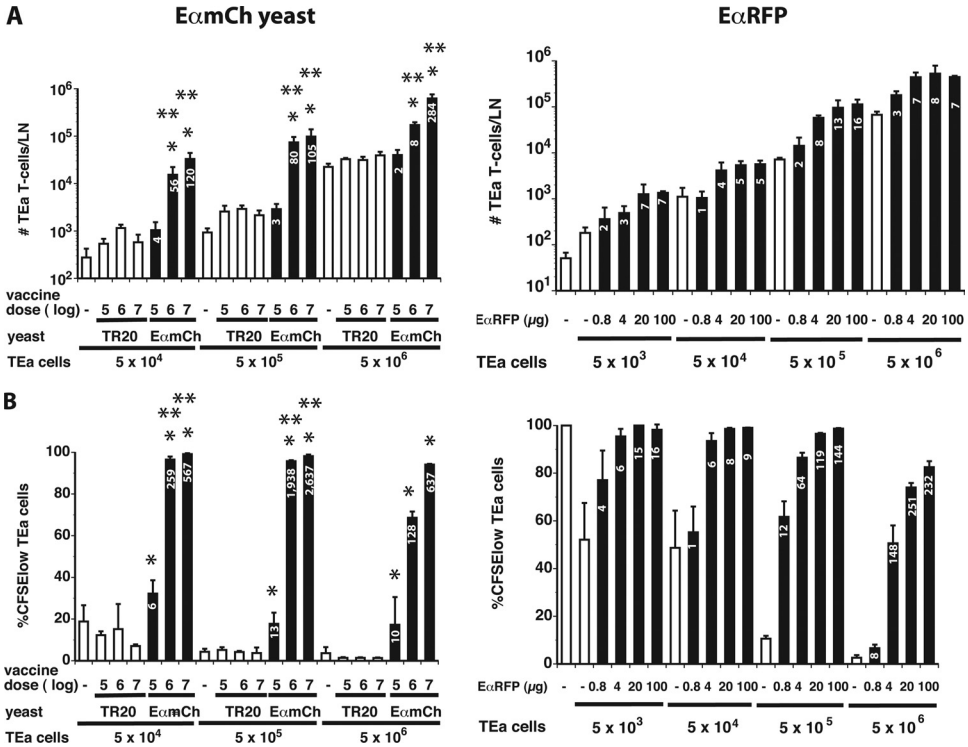

FIG 3 Impact of T cell precursor frequency and dose of vaccine Ag on expansion of adoptively transferred TEa cells in draining lymph nodes. (A) Crisscross titration of TEa cells and vaccine dose. TEa cells were labeled with CFSE and transferred into Thy1.2$^+$ congenic recipients at cell frequencies starting at 5×10^6 per recipient and decreasing by 10-fold. Thy1.1$^+$ CD4$^+$ cells were examined by cell surface staining and FACS analysis 4 days after vaccination with various doses of yeast (10^7, 10^6, and 10^5 Eα-mCh yeast) (left) or amounts of recombinant Eα-RFP from 0.8 μg to 100 μg (right). White numbers, *n*-fold increase in the number of TEa cells versus that in the corresponding ΔTR20-vaccinated group. (B) The number, percentage, and expansion of TEa cells that proliferated (CFSE^{lo}) were determined by FACS analysis. White numbers, *n*-fold increase in the number of TEa cells versus that in the corresponding group vaccinated with ΔTR20. The data represent averages $\pm$ SEMs of 4 mice per group from one representative experiment. The experiment was repeated twice with similar results. *, $P < 0.05$ versus unvaccinated- and ΔTR20-vaccinated groups; **, $P < 0.05$ versus corresponding 10^5 Eα-mCh yeast-vaccinated group.

results seen with a lysate of *E. coli* cells that express recombinant Eα-RFP-DsRed (25) or with His-tagged Eα-RFP purified from *E. coli* (data not shown). Importantly, Eα-mCh yeast cocultured with DC *in vitro* triggered activation and cytokine production in naïve and primed TEa cells when the T cells were added to cell culture wells (Fig. 2B). Thus, the DCs process and present Ag in Tg vaccine yeast and display model Eα peptide that can be detected within MHC-II on the DC surface by Y-Ae MAb, and these pEα–I-A^b complexes trigger Ag-specific T cells *in vitro*.

In view of these *in vitro* results, we undertook *in vivo* studies to explore activation, expansion, and tracking of TEa T cells after administration of Eα-mCh yeast vaccine (Fig. 2C). Here, we adoptively transferred 5×10^6 Thy1.1 TEa cells into Thy1.2 congenic mice 2 h before vaccination. Four days later, T cells from draining lymph nodes and spleen were analyzed. Controls included the TR20 strain lacking the transgene (ΔTR20; negative control) and the purified Eα-RFP (positive control). Vaccination with Eα-mCh yeast specifically activated and expanded TEa T cells in the node and spleen. About 68 to 70% of the Thy1.1 TEa cells expressed the activation marker CD44 and proliferated (defined by loss of CFSE) (Fig. 2C). The results were similar after vaccination with the positive control, Eα-RFP. In contrast, vaccination with the negative-control yeast expressing only the ΔTR20-BAD1 fusion partner (lacking Eα-mCh) failed to activate TEa T cells.

Impact of precursor frequency and vaccine dose on T cell expansion and activation. The number of transferred Tg T cells and amount of available Ag can impact expansion and activation of naïve precursor cells (1, 17). To determine the optimal conditions for T cell activation and expansion, we determined by crisscross titration the frequency of naïve TEa precursors with the vaccine dose of recombinant yeast and protein. Decreasing numbers of TEa cells were transferred into recipients on the day of vaccination, and the expansion of these cells was assessed in the draining lymph nodes 4 days after vaccination (peak of expansion; data not shown) using a dose range of 10^5 to 10^7 vaccine yeast or 0.8 μg to 100 μg of Eα-RFP. Expansion and activation of TEa cells were assessed by calculating the number of total CFSE^{low} and CD44$^+$ Thy1.1$^+$ cells. Independent of the transferred frequency, >80% TEa precursors became activated (data not shown) and expanded in a vaccine dose-dependent and Ag-specific manner (Fig. 3A and B). TEa cells showed significantly greater activation and expansion in mice vaccinated with 10^6 or 10^7 Eα-mCh yeast than mice vaccinated with 10^5 Eα-mCh yeast, TR20 yeast, or no vaccine. Even though TEa cell activation and expansion were the greatest with the highest vaccine dose, they approached a plateau with a dose of 10^6 Tg yeast. The precursor frequency of 5×10^5 TEa cells yielded the greatest T cell activation and expansion.

At a high precursor frequency, the amount of Ag may be limiting, thus reducing T cell activation and expansion. However, at

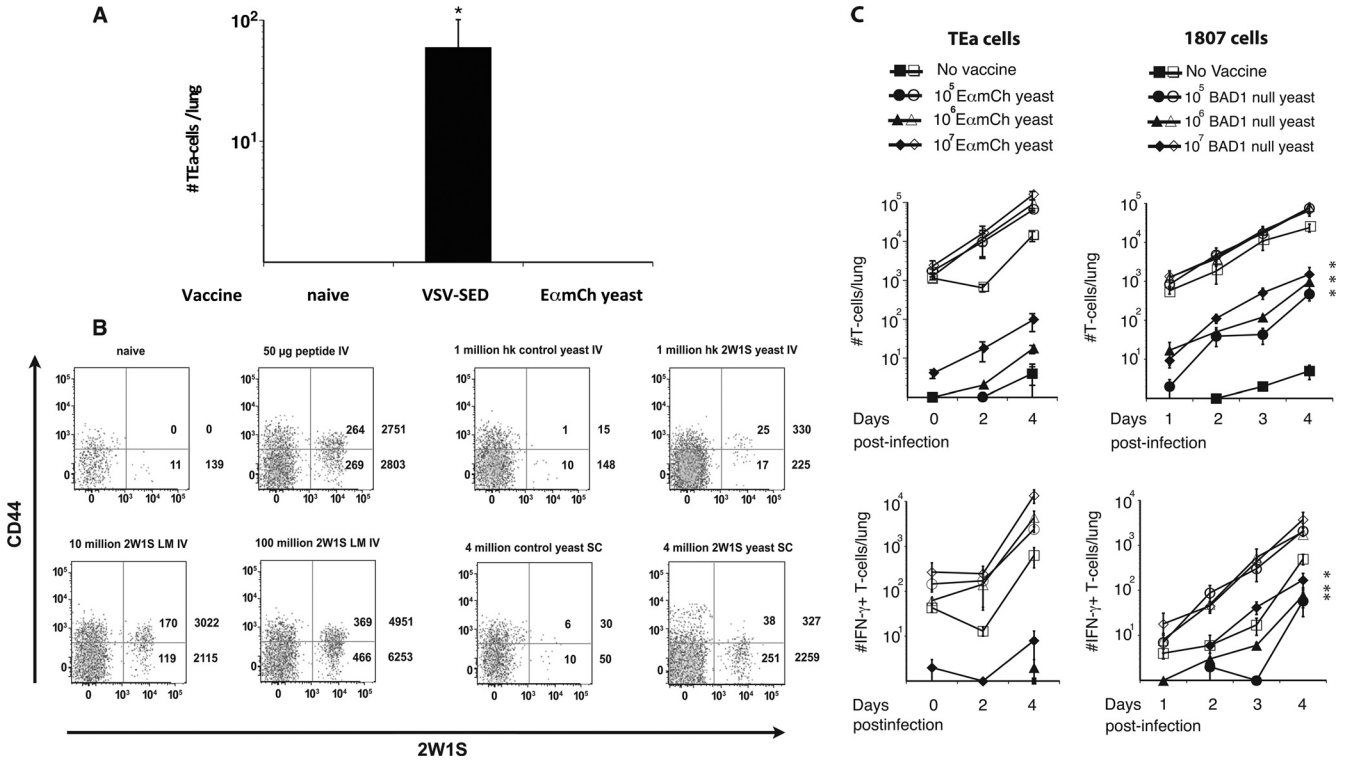

FIG 4 Role of Ag vehicle and identity on T cell activation, memory, and recall. (A) Recall of TEa cells to the lung after vaccination with VSV-SED. TEa cells (10^5) were adoptively transferred, and congenic recipient mice were vaccinated with 10^5 (i.v.) or 10^7 (s.c.) Eα-mCh yeast cells. Mice were challenged with 2×10^3 recombinant Eα-mCh ATCC 26199 yeast cells. The total number of TEa cells was calculated and graphed. *, $P < 0.05$ versus the number of TEa cells from mice vaccinated s.c. with Eα-mCh yeast. (B) Expansion and activation of endogenous Ag-specific $CD4^+$ T cells using 2W1S Tg vaccine yeast. Mice were vaccinated s.c. or i.v. with 1×10^6 or 4×10^6 recombinant 2W1S-expressing yeast cells or BAD1-null yeast cells (negative control), 10×10^6 or 100×10^6 recombinant 2W1S-expressing *L. monocytogenes* cells, or 50 μg 2W1S peptide plus 5 μg LPS administered i.v. At 7 days postvaccination, the skin-draining lymph nodes and spleen were harvested, tetramer and magnetic bead enriched, and analyzed for CD44 expression. The numbers inside the dot plots indicate the number of actual events recorded by FACS analysis, and the numbers outside the box indicate the calculated number of tetramer-positive cells per mouse hk, heat killed. (C) Recall of TEa and 1807 cells to the lung and cytokine production by the cells. At 4 weeks after vaccination, mice were challenged i.t. with 2×10^3 wild-type ATCC 26199 yeast cells, and at serial time points, lung T cells were analyzed for intracellular IFN-γ. The numbers of IFN-γ-producing TCR Tg cells (filled icons) and polyclonal, endogenous $CD4^+$ cells (open icons) were calculated and graphed. *, $P < 0.05$ versus TEa cells harvested from mice vaccinated with 10^5, 10^6, and 10^7 Eα-RFP yeast cells at days 2 and 4 postinfection.

lower precursor frequencies, in the absence of Eα Ag (e.g., the no-vaccine group), the number of TEa cells approaches the limit of detection, making the calculations for T cell expansion less accurate. Thus, we also calculated the ratio of total expanded TEa cells in mice that were vaccinated with the same dose and regimen but received log dilutions of TEa cell precursors. We calculated these ratios only for the two highest vaccine doses (10^6 and 10^7 yeast) since they drove significant expansion. The differences in TEa numbers were 5- to 6-fold less in Eα-mCh yeast-vaccinated mice that received 5×10^6 precursors than in those vaccinated with 5×10^5 precursors, indicating that TEa cells expanded relatively more at the lower precursor frequency (data not shown); in contrast, the relative expansion of TEa cells in mice that received 5×10^5 versus 5×10^4 precursors was nearly 10-fold, indicating that the lower precursor frequency did not yield increased proliferation. Thus, adoptive transfer of 1×10^5 to 5×10^5 TEa cells yielded maximal expansion, whereas a plateau was reached with transfer at higher frequencies.

Vaccination with Eα-RFP at ≥4 μg yielded maximal TEa cell activation and expansion, whereas a dose of 0.8 μg was limiting. Similar to yeast vaccination, TEa cells expanded most when they were transferred at a frequency of 5×10^5 precursors, likely for the reasons noted above. On the basis of these findings, in subsequent experiments, we chose to transfer 1×10^5 to 5×10^5 TEa cells unless otherwise stated, and we vaccinated mice with 10^6 Eα-mCh yeast or 20 μg of Eα-RFP because those doses induced maximal proliferation and activation at this precursor frequency.

Migration of antifungal TEa cells to lung upon recall. To see if primed antifungal TEa cells are functional during challenge and migrate to the lung and express cytokine, we analyzed the influx of Tg $CD4^+$ T cells at 4 days postinfection. Few to no TEa cells migrated to the lungs when we transferred 10^5 naïve Tg cells prior to vaccination (Fig. 4A). Since effector T cell development requires higher Ag loads than proliferation (18, 20), we speculated that the deficits of primed TEa cells described above might stem from a limited amount or duration of Eα Ag presentation. To test this idea, mice that received 10^5 naïve TEa cells were vaccinated i.v. with 10^5 VSV expressing Eα peptide (4). These conditions are known to induce TEa cell proliferation and promote memory development (4). Here, we found that TEa cells elicited by the VSV-SED vaccine were recruited to the lung on heterologous challenge with *Blastomyces* Eα-mCh yeast (Fig. 4A), indicating that functional TEa memory can develop if sufficient Ag is present during priming. These results suggest that Eα peptide is expressed by

recombinant yeast, but perhaps in amounts too small to promote the development of functional memory. Nevertheless, the amount of Eα peptide expressed by wild-type Eα-mCh yeast upon lung rechallenge was sufficient to recruit T cells initially primed by VSV-SED but not Eα-mCh yeast. Thus, it is possible that the amount of Eα peptide expressed by *Blastomyces* Tg yeast limited the initial priming but not the recruitment of already primed TEa cells during the recall response.

Expansion and activation of endogenous Ag-specific CD4$^+$ T cells by recombinant yeast. The preceding studies required adoptive transfer of relatively large numbers of Ag-specific T cells from TCR Tg mice. In that approach, T cells may receive less intense stimulation when present in large numbers due to intraclonal competition and the limiting amounts of Ag available per naïve T cell precursor (1, 4, 17, 24). To see if poor T cell recall to the lung and function may be due to the limiting amount of recombinant Ag expressed by *Blastomyces* yeast, we investigated the activation and expansion of an endogenous Ag-specific CD4$^+$ T cell. We engineered yeast that expresses 2W1S peptide (29). Tetramer-based enrichment recently showed the pool size of naïve 2W1S–I-A^b-specific CD4$^+$ T cells in C57BL/6 mice to be 190 precursors in the spleen and lymph nodes (27). An i.v. injection of 2W1S peptide plus LPS increased the population of 2W1S–I-A^b-specific T cells 300-fold to a peak of ~80,000 cells by day 6 (27).

To see if 2W1S-expressing yeast induced proliferation and activation of corresponding endogenous Ag-specific CD4$^+$ T cells, we vaccinated mice s.c. with live yeast or i.v. with heat-killed yeast that expresses surface 2W1S. As positive controls, mice were vaccinated with 50 μg 2W1S peptide plus LPS- or 2W1S-expressing *L. monocytogenes*. The spleen and draining nodes were harvested and tetramer enriched, and the number and activation of 2W1S tetramer-positive cells were analyzed (26, 27). Vaccination with 2W1S peptide plus LPS or recombinant *L. monocytogenes* increased the numbers of total and CD44^{hi} tetramer-positive cells by 40- and 80-fold, respectively, compared to those for naïve mice (Fig. 4B). In contrast, s.c. or i.v. vaccination with yeast expressing 2W1S increased the number of tetramer-positive cells by 32- and 3.4-fold compared to that for control vaccine yeast. Remarkably, only 15% $\pm$ 2% of the tetramer-positive cells showed increased surface expression of CD44 after s.c. vaccination with recombinant yeast, suggesting that the primed cells had not been fully activated. Although Ag-specific T cells expanded less in mice vaccinated i.v. with recombinant yeast, about half of the tetramer-positive cells expressed elevated CD44. Similarly, about half of the tetramer-positive cells in the groups vaccinated with peptide or recombinant *L. monocytogenes* exhibited an activated phenotype (CD44^{hi}). Thus, 2W1S yeast did modestly expand endogenous Ag-specific CD4$^+$ T cells, but the activation state of these T cells was surprisingly low, as measured by CD44 expression.

Migration of vaccine-induced 1807 cells into lung upon challenge. The preceding studies with Tg yeasts expressing Eα and 2W1S suggest that low antigen expression may have limited the development of effector T cells. To investigate whether endogenous fungal antigens prime naïve CD4$^+$ T cells more efficiently than the model antigens, we adoptively transferred naïve *B. dermatitidis*-specific 1807 cells into mice prior to vaccination with BAD1-null yeasts that do not express model antigens (6, 37). Comparable numbers of polyclonal CD4$^+$ T cells migrated into the lungs after challenge and expressed gamma interferon (IFN-γ) in mice that had received adoptively transferred TEa or 1807 cells and were vaccinated with Eα-mCh yeast or BAD1-null yeast (Fig. 4C). In contrast, 10-fold fewer antifungal TEa cells than 1807 cells migrated into the lung and produced cytokine. Thus, the limited recall response by model Ag-specific TEa cells was not observed with endogenous yeast Ag-specific 1807 cells.

Effect of Ag dose and duration on recall and function of primed TEa cells. To further explore the impact of Ag limitation on the recall response to the lung, we took a third approach. We regulated the dose of Ag by providing supplemental Eα protein with Eα-mCh yeast vaccine, and we prolonged the duration of Ag delivery by emulsifying Eα-RFP in IFA. Eα-RFP emulsified in IFA induced the maximal generation of effector/memory cells in the draining lymph nodes at 5 weeks postvaccination (Fig. 5A). The addition of Eα-RFP alone or with IFA to mice vaccinated with Eα-mCh yeast also increased the number of effector TEa cells in the draining nodes. However, the lung recall response was weak after vaccination with Eα-RFP plus IFA, similar to that after vaccination with Eα-mCh yeast (Fig. 5B). The addition of exogenous Eα-RFP alone or in conjunction with IFA to the Eα-mCh vaccine significantly enhanced the numbers of IFN-γ- and IL-17-producing TEa cells upon lung recall. These results indicate that Ag dose and duration influence the quantity and quality of the TEa recall response and illustrate that the amount of model Ag expressed by the recombinant vaccine is likely insufficient to drive an efficient recall of TEa effector cells into the lung. However, vaccination with Eα-RFP alone was insufficient to induce maximal responses, and Tg yeast in conjunction with high Ag loads delivered by Eα-RFP led to maximal recruitment of TEa effectors to the lung.

To investigate whether a lack of secondary expansion upon lung rechallenge contributes to the reduced numbers of TEa cells in mice vaccinated with Eα-mCh yeast, we measured TEa cell proliferation in the lung and MLN at day 4 postinfection. In all three groups of vaccinated mice (mice vaccinated with TR20, Eα-mCh, and Eα-mCh–Eα-RFP–IFA), >90% of the CD44$^+$ CD62L^{low} TEa cells in the lung and MLN underwent proliferation, as measured by BrdU staining (Fig. 5C). Similarly, >90% of activated 1807 cells from vaccinated mice underwent secondary proliferation in the lung and MLN upon rechallenge. Since BrdU incorporation does not indicate the number of cell divisions, we cannot exclude the possibility that T cells expanded to different degrees among the vaccine groups. Interestingly, we observed an inverse relationship between the number of proliferated and activated T cells in the lung versus the MLN among the different groups of mice. Mice vaccinated with Eα-mCh–Eα-RFP–IFA or BAD1-null yeast showed efficient recruitment and/or secondary expansion of TEa and 1807 cells into the lung but poor secondary expansion into the MLN. On the other hand, poor recruitment of T cells into the lungs of Eα-mCh yeast-vaccinated mice or unvaccinated mice was accompanied by increased secondary expansion in the MLN. In summary, recruitment and/or secondary expansion is the determining factor for the number of TEa and 1807 cells found in the lung of rechallenged mice.

DISCUSSION

An understanding of the factors that influence Ag presentation, priming of Ag-specific T cells, and memory T cell development is essential for the rational design of vaccines. In work described here, we sought to establish a heterologous adoptive transfer system to quantitatively and qualitatively monitor the development

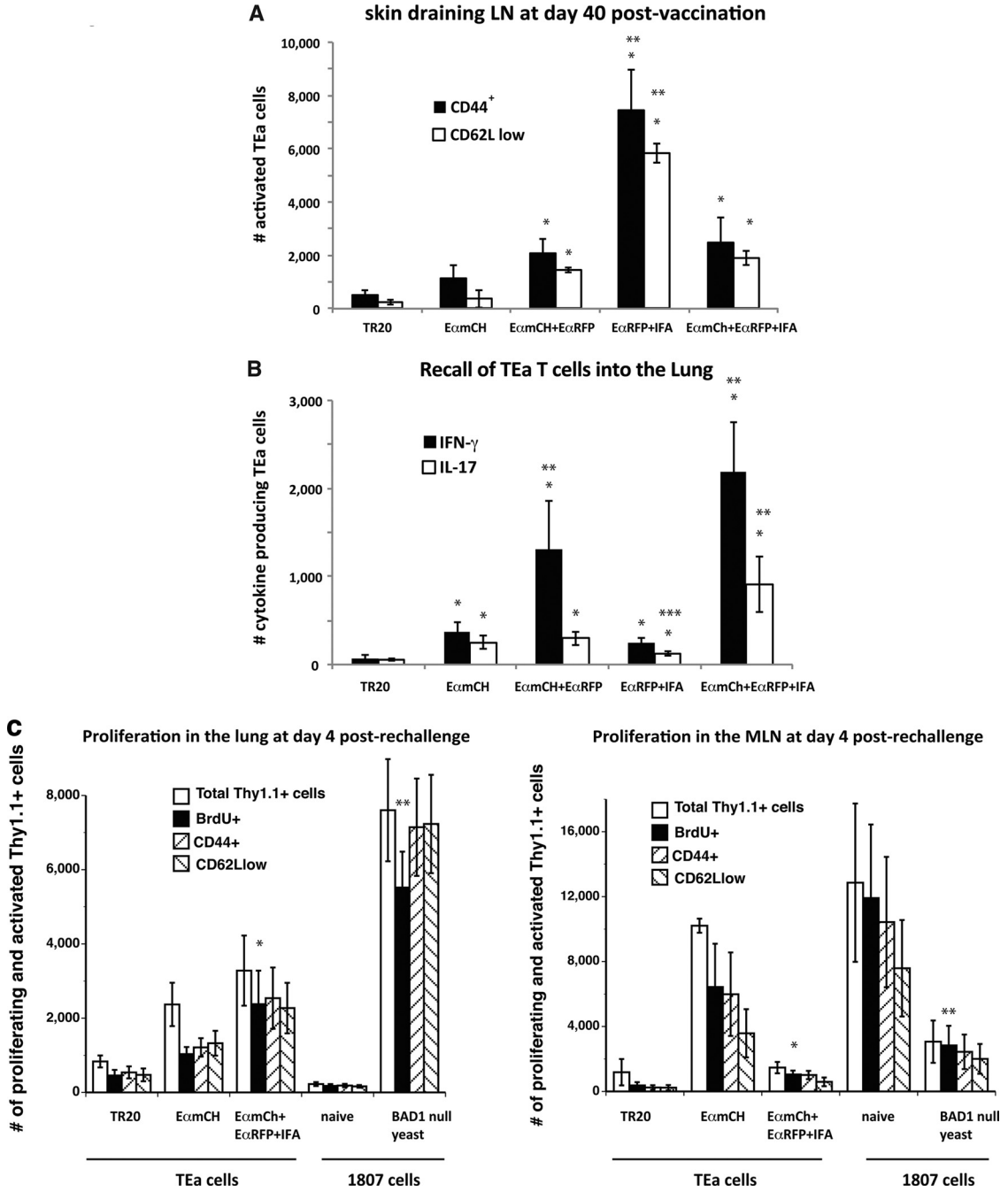

FIG 5 Influence of Ag dose and duration on TEa cell activation, memory, and recall. (A) Effector/memory TEa cells in skin-draining lymph nodes at 6 weeks postvaccination. TEa cells (10^6) were adoptively transferred, and recipient mice were vaccinated with 10^7 Eα-mCh yeast cells alone, Eα-mCh yeast cells mixed with 100 μg Eα emulsified with IFA, or Eα-mCh yeast cells plus 100 μg Eα-RFP and IFA. Six weeks later, the skin-draining lymph nodes were harvested and TEa cells were analyzed by FACS analysis. The data represent averages ± SEMs of 4 to 6 mice per group from one representative experiment. The experiment was repeated twice with similar results. *, $P < 0.05$ versus ΔTR20-vaccinated group, **, $P < 0.05$ versus all other groups. (B) Recall of TEa cells into the lung at 4 days postinfection. Mice received TEa cells and were vaccinated as described for panel A. At 5 weeks postvaccination, the mice were challenged with 2×10^4 Eα-mCh-expressing wild-type (ATCC 26199) yeast cells. The number of cytokine-producing TEa cells was determined by FACS analysis. The data represent averages ± SEMs of 6 to 8 mice per group from two independent experiments. *, $P < 0.05$ versus ΔTR20 group; **, $P \leq 0.05$ versus Eα-mCh yeast and Eα-RFP–IFA groups; ***, $P < 0.05$ versus Eα-mCh group. (C) Proliferation of T cells in the lung and MLN postchallenge. Mice were vaccinated as described for panel A and challenged with 2×10^4 Eα-mCh-expressing wild-type yeast cells. On the day of challenge and daily thereafter, mice received BrdU i.p. At 4 days postinfection, the mice were sacrificed and the number of BrdU-positive T cells was determined by FACS analysis. The data represent averages ± SEMs of 4 to 5 mice per group from one representative out of two independent experiments. *, $P < 0.05$ versus number of BrdU-positive TEa cells in groups vaccinated with ΔTR20 or Eα-mCh yeast; **, $P \leq 0.05$ versus number of BrdU-positive cells in the unvaccinated group.

of fungus-specific CD4$^+$ T cell memory. To establish a system to study antifungal CD4$^+$ T cell development *in vivo*, we performed extensive testing of the variables that influence T cell phenotypes and function. It is now recognized that the input frequency of naïve TCR Tg precursors and the availability of Ag are the most important factors that dictate the fate of T cell development. A high level of initial TCR Tg precursor has frequently led to an intrinsic defect in the T cells and resulted in reduced division, altered kinetics of expansion, reduced cytokine production, and the lack of a detectable memory population (4, 17, 21, 24). In those studies, T cell competition could be overcome by adding more Ag (7, 34) or Ag-bearing APCs (36). Below, we discuss our results obtained using a heterologous, adoptive transfer system to study antifungal CD4$^+$ T cell immunity. We analyzed selected stages of the antifungal T cell response, including activation, proliferation, differentiation, memory, and migration to the lung upon a recall challenge.

We found that Eα-mCh expressed on vaccine yeasts did not impair their ability to confer resistance and that transgene expression on wild-type yeast did not impair their virulence during rechallenge (data not shown). Eα-mCh on yeast was processed and presented on APCs, and the peptide triggered the activation and proliferation of corresponding TEa cells in an Ag-specific manner. TEa cells expanded maximally using an input precursor frequency of 5×10^5 Tg cells and a vaccine dose of 10^6 to 10^7 yeast cells. Transfer of $\leq 5 \times 10^3$ TEa precursors did not yield a detectable number of primed TEa cells in the skin-draining lymph nodes at the burst of expansion (at day 7 postvaccination). Fungus-specific TEa cells expanded a maximum of 1,000- to 3,000-fold using a precursor frequency of 5×10^5 naïve cells and less than 1,000-fold using higher and lower precursor frequencies (Fig. 3A). It is conceivable that the expansion of 5×10^4 TEa precursors might have been higher than we calculated since the number of TEa cells in the unvaccinated group was near the detection limit, and therefore, the calculations of the *n*-fold expansion factor might not have been as precise as in the higher-precursor-frequency groups. Thus, 5×10^4 to 5×10^5 TEa precursors had to be transferred to yield a measurable pool of primed TEa cells at the peak T cell response in the skin-draining lymph nodes.

Antifungal TEa cells primed with Eα-mCh yeast alone failed to efficiently acquire memory and migrate to the lung upon challenge. In contrast, adoptive transfer of comparable numbers (1×10^5 to 5×10^5) of 1807 cells that recognize an endogenous fungal antigen led to the induction of memory and recruitment of effector cytokine-producing 1807 cells into the lung (Fig. 4C). We hypothesize that the amount of Eα peptide expressed by vaccine yeast and/or the duration of Ag presentation was sufficient to induce proliferation, but not differentiation and memory development. This idea is compatible with earlier reports indicating that the signaling threshold for proliferation of naïve T cells is lower than the threshold necessary to drive the differentiation of memory cells (4). Ag limitation characterized by the amount of Ag available per T cell precursor can be the result of transferring too many initial precursor T cells into recipient mice or limited availability of the cognate Ag. However, we found that reducing the precursor frequency to 10^4 naïve TEa cells and enriching the cells with magnetic beads (17) at the time of harvest did not yield sufficient numbers of trackable TEa cells (data not shown). Rather, we found that delivery of recombinant VSV-SED vaccine restored TEa functions, indicating that the vehicle (virus versus fungus) and/or the delivery route (i.v. versus s.c.) critically impacts the levels of Ag available per naïve T cell precursor. Interestingly, VSV-SED-primed TEa cells were efficiently recruited to the lung in response to rechallenge with Eα-mCh yeast. These results suggest that the antigen threshold for recruiting already primed TEa cells is lower than it is for TEa cells initially primed naïve during vaccination.

To verify that poor TEa recall resulted from limited Ag expression by recombinant Eα-mCh vaccine yeast, we added exogenous Eα-RFP to the vaccine yeast. The addition of Eα-RFP alone or with IFA significantly boosted the number of cytokine-producing TEa cells that migrated to the lung and expanded upon challenge, whereas administration of just Eα-RFP plus IFA (without yeast) yielded poor recall responses and secondary expansion in the lung. These results are consistent with our hypothesis that the amount of Ag expressed by Eα-mCh yeast alone during vaccination limited the quality and quantity of functional memory TEa cells. However, because vaccine yeast added to Eα-RFP enhanced lung recall, our results also highlight the fact that the yeast is a potent adjuvant for inducing functional effector T cells.

We used an additional strategy to exclude the possibilities that the high frequency of transferred cells or the identity of the model Ag may have skewed our results. Here, we controlled for the means of Ag expression (yeast) while changing the antigen and using tetramer staining to track endogenous T cells. We engineered yeasts that express the 2W1S peptide, an epitope that is recognized by the most frequent population of endogenous Ag-specific CD4$^+$ T cells known to date (27). The expansion and activation of 2W1S tetramer-positive T cells in response to vaccination with recombinant yeast were modest compared to those in response to vaccination with recombinant *L. monocytogenes* infection, and the population of primed (CD44$^+$) 2W1S-specific T cells was too small to evaluate memory and recall functions. This result supports our interpretation that the amount of yeast-displayed model Ag was limiting and did not exceed the necessary threshold.

We conclude that the heterologous adoptive transfer system described here is a powerful method to study the earliest events of Ag presentation to antifungal CD4$^+$ T cells. We showed that Y-Ae MAb nicely detected yeast-derived Eα–pMHC-II complexes on DCs. These levels of Ag display corresponded with robust T cell activation, proliferation, and expansion of antifungal CD4$^+$ TEa cells during the first week after vaccination. However, the downstream effector, memory, and recall functions of TEa cells were blunted by insufficient Ag display on the vaccine yeast. Thus, this TEa Tg system is ideally suited to studying fungal Ag presentation and early T cell priming, whereas T cell effector and memory development may instead be studied with the autologous TCR Tg 1807 cells described recently (37).

ACKNOWLEDGMENTS

We thank Roger Tsien from the University of California at San Diego for provided the clone sequence for the mCherry gene.

This work was supported by NIH grants R21 AI076700 (to M.W.) and R01 AI40996 (to B.S.K.).

REFERENCES

1. **Badovinac VP, Haring JS, Harty JT.** 2007. Initial T cell receptor transgenic cell precursor frequency dictates critical aspects of the CD8(+) T cell response to infection. Immunity **26**:827–841.
2. **Beijersbergen A, Dulk-Ras AD, Schilperoort RA, Hooykaas PJ.** 1992.

Conjugative transfer by the virulence system of Agrobacterium tumefaciens. Science **256**:1324–1327.
3. **Bernard P, Couturier M.** 1992. Cell killing by the F plasmid CcdB protein involves poisoning of DNA-topoisomerase II complexes. J. Mol. Biol. **226**: 735–745.
4. **Blair DA, Lefrancois L.** 2007. Increased competition for antigen during priming negatively impacts the generation of memory CD4 T cells. Proc. Natl. Acad. Sci. U. S. A. **104**:15045–15050.
5. **Brandhorst TT, Gauthier GM, Stein RA, Klein BS.** 2005. Calcium binding by the essential virulence factor BAD-1 of Blastomyces dermatitidis. J. Biol. Chem. **280**:42156–42163.
6. **Brandhorst TT, Wüthrich M, Warner T, Klein B.** 1999. Targeted gene disruption reveals an adhesin indispensable for pathogenicity of Blastomyces dermatitidis. J. Exp. Med. **189**:1207–1216.
7. **Catron DM, Rusch LK, Hataye J, Itano AA, Jenkins MK.** 2006. CD4+ T cells that enter the draining lymph nodes after antigen injection participate in the primary response and become central-memory cells. J. Exp. Med. **203**:1045–1054.
8. **Cutler JE, Deepe GS, Jr, Klein BS.** 2007. Advances in combating fungal diseases: vaccines on the threshold. Nat. Rev. Microbiol. **5**:13–28.
9. **De Boer RJ, Homann D, Perelson AS.** 2003. Different dynamics of CD4+ and CD8+ T cell responses during and after acute lymphocytic choriomeningitis virus infection. J. Immunol. **171**:3928–3935.
10. **den Dulk-Ras A, Hooykaas PJ.** 1995. Electroporation of Agrobacterium tumefaciens. Methods Mol. Biol. **55**:63–72.
11. **Ertelt JM, et al.** 2009. Selective priming and expansion of antigen-specific Foxp3-CD4+ T cells during Listeria monocytogenes infection. J. Immunol. **182**:3032–3038.
12. **Fabien N, Bergerot I, Maguer-Satta V, Orgiazzi J, Thivolet C.** 1995. Pancreatic lymph nodes are early targets of T cells during adoptive transfer of diabetes in NOD mice. J. Autoimmun. **8**:323–334.
13. **Firpo EJ, et al.** 2002. Antigen-specific dose-dependent system for the study of an inheritable and reversible phenotype in mouse CD4+ T cells. Immunology **107**:480–488.
14. **Fisher LD, van Belle G.** 1993. Biostatistics: a methodology for the health sciences, p 611–613. John Wiley & Sons, New York, NY.
15. **Grubin CE, Kovats S, deRoos P, Rudensky AY.** 1997. Deficient positive selection of CD4 T cells in mice displaying altered repertoires of MHC class II-bound self-peptides. Immunity **7**:197–208.
16. **Harvey RP, Schmid ES, Carrington CC, Stevens DA.** 1978. Mouse model of pulmonary blastomycosis: utility, simplicity, and quantitative parameters. Am. Rev. Respir. Dis. **117**:695–703.
17. **Hataye J, Moon JJ, Khoruts A, Reilly C, Jenkins MK.** 2006. Naive and memory CD4+ T cell survival controlled by clonal abundance. Science **312**:114–116.
18. **Iezzi G, Karjalainen K, Lanzavecchia A.** 1998. The duration of antigenic stimulation determines the fate of naive and effector T cells. Immunity **8**:89–95.
19. **Itano AA, et al.** 2003. Distinct dendritic cell populations sequentially present antigen to CD4 T cells and stimulate different aspects of cell-mediated immunity. Immunity **19**:47–57.
20. **Jelley-Gibbs DM, Lepak NM, Yen M, Swain SL.** 2000. Two distinct stages in the transition from naive CD4 T cells to effectors, early antigen-dependent and late cytokine-driven expansion and differentiation. J. Immunol. **165**:5017–5026.
21. **Kemp RA, Powell TJ, Dwyer DW, Dutton RW.** 2004. Cutting edge: regulation of CD8+ T cell effector population size. J. Immunol. **173**:2923–2927.
22. **Lara-Tejero M, Pamer EG.** 2004. T cell responses to Listeria monocytogenes. Curr. Opin. Microbiol. **7**:45–50.
23. **Lefebvre B, Formstecher P, Lefebvre P.** 1995. Improvement of the gene splicing overlap (SOE) method. Biotechniques **19**:186–188.
24. **Marzo AL, et al.** 2005. Initial T cell frequency dictates memory CD8+ T cell lineage commitment. Nat. Immunol. **6**:793–799.
25. **Matz MV, et al.** 1999. Fluorescent proteins from nonbioluminescent Anthozoa species. Nat. Biotechnol. **17**:969–973.
26. **Moon JJ, et al.** 2009. Tracking epitope-specific T cells. Nat. Protoc. **4**:565–581.
27. **Moon JJ, et al.** 2007. Naive CD4(+) T cell frequency varies for different epitopes and predicts repertoire diversity and response magnitude. Immunity **27**:203–213.
28. **Nemecek JC, Wüthrich M, Klein BS.** 2006. Global control of dimorphism and virulence in fungi. Science **312**:583–588.
29. **Rees W, et al.** 1999. An inverse relationship between T cell receptor affinity and antigen dose during CD4(+) T cell responses in vivo and in vitro. Proc. Natl. Acad. Sci. U. S. A. **96**:9781–9786.
30. **Romani L.** 2004. Immunity to fungal infections. Nat. Rev. Immunol. **4**:1–23.
31. **Rudensky A, Rath S, Preston-Hurlburt P, Murphy DB, Janeway CA, Jr.** 1991. On the complexity of self. Nature **353**:660–662.
32. **Shaner NC, et al.** 2004. Improved monomeric red, orange and yellow fluorescent proteins derived from Discosoma sp. red fluorescent protein. Nat. Biotechnol. **22**:1567–1572.
33. **Singh A, Wuthrich M, Klein B, Suresh M.** 2007. Indirect regulation of CD4 T-cell responses by tumor necrosis factor receptors in an acute viral infection. J. Virol. **81**:6502–6512.
34. **Smith AL, Wikstrom ME, Fazekas de St Groth B.** 2000. Visualizing T cell competition for peptide/MHC complexes: a specific mechanism to minimize the effect of precursor frequency. Immunity **13**:783–794.
35. **Sullivan TD, Rooney PJ, Klein BS.** 2002. Agrobacterium tumefaciens integrates transfer DNA into single chromosomal sites of dimorphic fungi and yields homokaryotic progeny from multinucleate yeast. Eukaryot. Cell **1**:895–905.
36. **Willis RA, Kappler JW, Marrack PC.** 2006. CD8 T cell competition for dendritic cells in vivo is an early event in activation. Proc. Natl. Acad. Sci. U. S. A. **103**:12063–12068.
37. **Wüthrich M, Ersland K, Galles KJ, Sullivan TD, Klein BS.** Fungi subvert vaccine T-cell priming at the respiratory mucosa by inducing MMP2 and retarding CCL7-mediated influx of inflammatory monocytes. Immunity, in press.
38. **Wüthrich M, Filutowicz HI, Klein BS.** 2000. Mutation of the WI-1 gene yields an attenuated Blastomyces dermatitidis strain that induces host resistance. J. Clin. Invest. **106**:1381–1389.
39. **Wüthrich M, Filutowicz HI, Warner T, Deepe GS, Jr, Klein BS.** 2003. Vaccine immunity to pathogenic fungi overcomes the requirement for CD4 help in exogenous antigen presentation to CD8+ T cells: implications for vaccine development in immune-deficient hosts. J. Exp. Med. **197**:1405–1416.
40. **Wüthrich M, Filutowicz HI, Warner T, Klein BS.** 2002. Requisite elements in vaccine immunity to Blastomyces dermatitidis: plasticity uncovers vaccine potential in immune-deficient hosts. J. Immunol. **169**:6969–6976.
41. **Wüthrich M, Fisette PL, Filutowicz HI, Klein BS.** 2006. Differential requirements of T cell subsets for CD40 costimulation in immunity to Blastomyces dermatitidis. J. Immunol. **176**:5538–5547.
42. **Wüthrich M, et al.** 2011. Vaccine-induced protection against 3 systemic mycoses endemic to North America requires Th17 cells in mice. J. Clin. Invest. **121**:554–568.
43. **Wüthrich M, et al.** 2011. A TCR transgenic mouse reactive with multiple systemic dimorphic fungi. J. Immunol. **187**:1421–1431.
44. **Wüthrich M, Klein BS.** 2000. Investigation of anti-WI-1 adhesin antibody-mediated protection in experimental pulmonary blastomycosis. J. Infect. Dis. **181**:1720–1728.
45. **Wüthrich M, Warner T, Klein BS.** 2005. IL-12 Is required for induction but not maintenance of protective, memory responses to Blastomyces dermatitidis: implications for vaccine development in immune-deficient hosts. J. Immunol. **175**:5288–5297.